MULTI-DEVICE STUDY OF MHD MODES LOCKING IN TOKAMAKS

V. Klevarová[1], G. Pautasso[2], H. Zohm[2], P.C. de Vries[3], M. Lehnen[3], T. Markovič[4,5], M. Komm[4], J. Havlíček[4], G. Verdoolaege[1,6], JET contributors*, the EUROfusion MST1 team+ and the ASDEX Upgrade team

INTRODUCTION

- Tearing modes are observed to cause disruptions in tokamaks, prior to the disruption onset, modes are either locked or rotating:

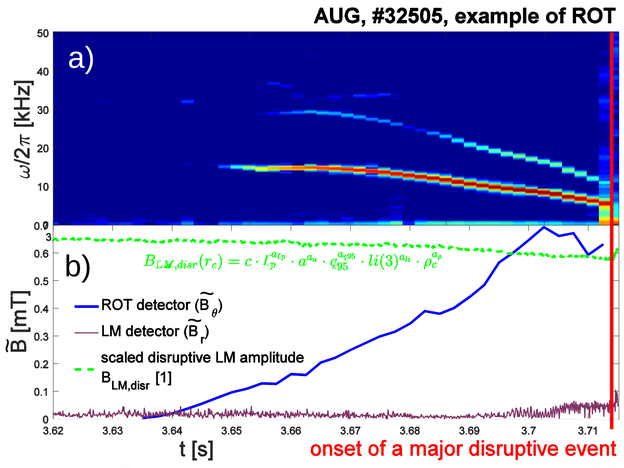

Fig.1 (a) Spectrogram showing the presence of disruptive ROT (b) mode amplitude measured by sensors sensitive to ROT/LM and the predicted LM disruptive amplitude [1]

ROT – rotating until disruption
ROT->LM – initially rotating mode, locked at the disruption onset
BLM – born-locked mode

- Multi-device database of disruptive discharges assembled, suitable for study of disruption precursors (Tab.1)
- Fraction of ROT/ROT->LM/BLM scales with device size
- In disruption prediction schemes, it might be desirable to implement amplitude of rotating modes, else risk of missing ROT (Fig.1)

DEVICE	# of database entries	a [m]	R_0 [m]	ROT/ROT->LM/BLM [%]
COMPASS	283	0.18	0.56	55/40/5
AUG full-W wall	457	0.50	1.65	21/56/23
JET-ILW	281	1.0	2.96	5/52/43

Tab.1 Parameters concerning the full multi-device database of disruptive discharges

- Different disruption avoidance techniques may be applied for ROT and LM

RQs
→ At what mode amplitude is locking initiated?
→ What determines the ROT/ROT->LM/BLM fraction in particular device?

- Answering RQs with the ROT/ROT->LM devices databases (> 150 COMPASS, > 220 AUG, > 40 JET cases) might help to estimate conditions for mode locking in ITER

MODE LOCKING MODEL

- Equation of mode motion comprises sum of all torques exerted on the island mass

$$I\frac{d\omega}{dt} = \sum T_\phi \longrightarrow \text{only toroidal motion assumed} \quad (1)$$

- Motion restoring viscous force F_{VS} and braking resistive wall force F_{RW} considered [2]

$$\frac{d\omega}{dt} = F_{VS} - F_{RW} = \frac{\omega_0}{\tau_{M0}} - \frac{\omega}{\tau_M} - A\left(\frac{w}{a}\right)^4 \frac{\omega\tau_w}{(\omega\tau_w)^2+m^2} \quad (2)$$

$F_{VS} = \frac{\omega_0-\omega}{\tau_{M0}} = \frac{\omega_0}{\tau_{M0}} - \frac{\omega^*}{\tau_M}$

In [2], $\tau_M = f\left(\frac{w}{a}\right) = \frac{\tau_{M0}}{1+B(\frac{w}{a})}$ is proposed, adopting model for $\tau_E \approx \tau_M$ degradation [3]

$F_{RW} \propto \left(\frac{w}{a}\right)^4$ as presented in [4], assuming the whole plasma decelerating with the mode+

$A = \frac{m^2}{256}\left(\frac{r_s}{r_w}\right)^{2m}\left(\frac{q'}{q}\right)^2_{r_s}\frac{a^2B_\theta^2(r_s)}{\mu_0 n_e m_i}\frac{2n^2}{R_0^2} = A_0/\tau_{a\theta}^2$

- Search for points of balanced forces, i.e. solutions of $\dot{\omega} = 0$, for increasing *{w/a}*

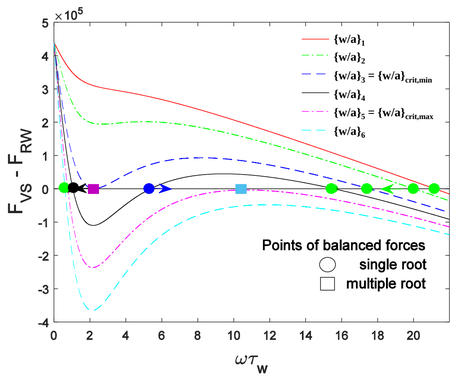

Fig.2 $F_{VS} - F_{RW}$ plotted for increasing {w/a}, shown as a function of dimensionless $\omega\tau_w$

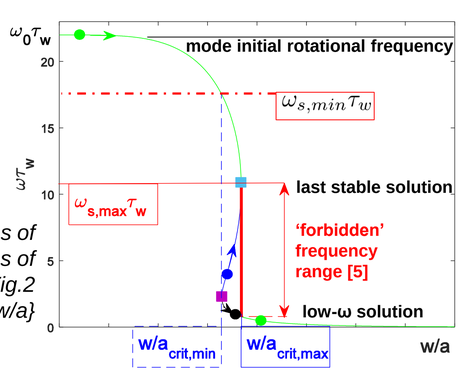

Fig.3 Trajectories of single&multiple solutions of (2) = 0 presented in Fig.2 shown for increasing {w/a}

→ multiple solutions ∃ for $\{w/a\} \in [\{w/a\}_{crit,min}\ \{w/a\}_{crit,max}]$, at $\{w/a\} = \{w/a\}_{crit,max}$ last stable solution is met and for further $\{w/a\}\nearrow$, mode decays from $\omega_{s,max}\tau_w$ to low-ω solution

- Condition of $\{w/a\}_{crit,max}$ ∃: $A\tau_M\tau_w(w/a)^4 > 8C$. For further $\{w/a\}\nearrow$, $A\tau_M\tau_w(w/a)^4 \gg 8C$ and

$$\left(\frac{w}{a}\right)^2\left(2+B\frac{w}{a}\right)\Big|_{crit,max} = \frac{\omega_0\tau_w}{\sqrt{A\tau_{M0}\tau_w}} \quad (3)\ B = 0 \rightarrow \boxed{\frac{w}{a}\Big|_{crit,max} = \frac{1}{\sqrt{2}}\,\omega_0^{1/2}\cdot\tau_{A\theta}^{1/2}\cdot\tau_w^{1/4}\cdot\tau_{M0}^{-1/4}\cdot A_0^{-1/4}} \quad (4)$$

- Example of integration of (2) for an AUG-like set of input parameters (Tab.2) is in Fig.4

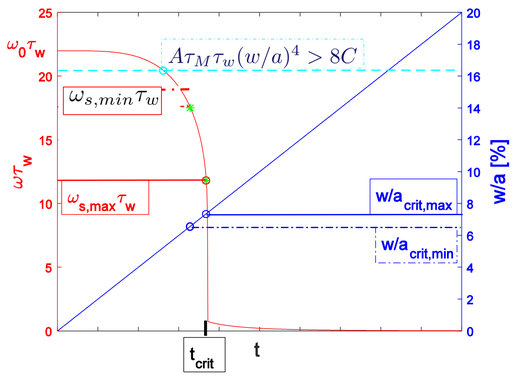

τ_w [ms]	q_{95}	R_0 [m]	$\omega_0/2\pi$ [kHz]	τ_{M0} [ms]	m/n
1.0	3.6	1.65	3.5	50	2/1
B	**I_p [MA]**	**B_T [T]**	**n_e [m^{-3}]**	**r_s/a**	
1.0	1.0	2.5	5.0e19	1.0	

Tab.2 AUG-like set of parameters submitted to (2) integration

Fig.4 Evolution of the mode rotational frequency prescribed by (2) for the AUG-like standard set, B = 0; island width growth was prescribed by $w/a = w/a_s(t/\tau)$

*plasma modeled as a rigid body, +derived for cylindrical plasma

COLLECTION AND VALIDATION OF EXPERIMENTAL DATA

- Formulas (2,4) incorporate device&discharge dependent parameters enabling direct comparison of experimental time traces with that predicted by the model
- **First, model applicability tested on AUG ROT/ROT->LM database entries**
  → necessary input for model test collected and validated:

Mode frequency and amplitude
→ tracked with help of spectrograms retrieved by set of Mirnov coils
$\bar{\omega_0}/2\pi|_{m=2} = 3.4 \pm 2.9$ kHz
$\bar{\omega_0}/2\pi|_{m=3} = 2.6 \pm 2.3$ kHz

Resistive wall time
→ set to inverse of typical growth rates of RWMs, i.e. τ_w = 10 ms

Island width
→ cylindrical formula for w calculation used, calibrated with ECE records
$w_{mag} = 4\sqrt{\frac{qr_s\tilde{B}}{mq'B_\theta}}_{r=r_s}$, $w_{ECE} \sim 1.2w_{mag}$

Mode m/n structure
→ retrieved with the help of phase fitting

m/n	2/1	3/1	4/1	other
% of cases	42	50	6	<2

MHD equilibrium reconstruction
→ for modes evolving in flat-top phase $q_0 = 1$ set, r_s compared with phase jump in ECE records

Momentum confinement time
→ retrieved for ~ 140 shots with TRANSP code, If unavailable, calibration $\tau_{M0} = 1.8 \cdot \tau_{E0}$ used

Plasma density
→ retrieved preferentially with HRTS records, if unavailable, with interferometer core LoS data

APPLICATION OF MODEL TO THE AUG EXPERIMENT

- AUG ROT/ROT->LM database is populated with various instabilities (explosively growing, immediately locking radiation-driven modes near the density limit (Fig.5a), quasi-stable NTMs (Fig.5b)..)

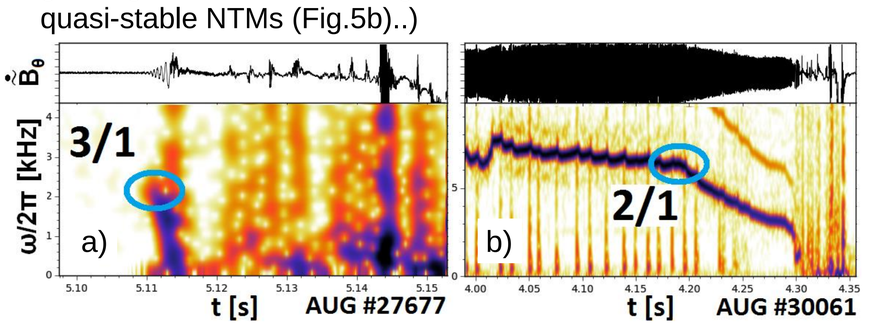

Fig.5 (a,b) Examples of ROT/ROT->LM AUG database entries, encircled are points of initiation of mode deceleration

- Median of rotation phase duration is ~ 23 ms, median growth rate (exponential or linear) ~ 6.0 ms^{-1} , 95 % of $w/a_{crit,max}$ evaluated with Eq.4 are within interval $w/a_{crit,max}$ ~ [7 28] %
- Median of braking resistive wall torque at the initiation of the mode slowing down phase ~ 0.06 Nm → torque too low to cause mode locking in *any* of the database entries, an example is shown in Fig.6
- Force balance (2) is incomplete and does not describe mode locking in AUG
  → resistive wall force is weak by a factor ~ 100
  → other braking terms (e.g. interaction with the intrinsic error fields) should be considered or existing to be modified

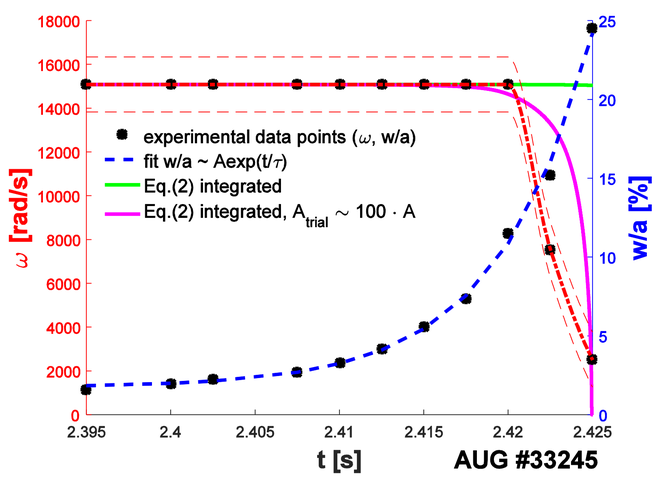

Fig.6 Experimental ω and w/a times traces, shown together with the result of integration of Eq.(2) for the respective input parameters. Note that the resulting ω = f(t) does not lock within the designated temporal window. Integration result approaches experimental points when a trial integration is performed, multiplying A by a factor ~ 100

* similar problem encountered in [6], addressing mode locking in DIII-D → authors proposed to include in F_{RW} a 2nd resistive wall, mimicked by in-vessel tiles, of $\tau_w \gg \tau_{tiles}$

SUMMARY & OUTLOOK

- Simple model for mode locking incorporating restoring viscous force and braking resistive wall force was used to characterize mode locking in AUG
- Model allows to define critical condition for mode locking exactly (Eq.4), calculated critical island sizes are in reasonable correspondence with experimental data points
- However, experimental time traces were not reproduced due to too weak a wall drag
- Model requires modification, in terms of adding braking force and/or modification of the already considered terms

REFERENCES

[1] P.C. de Vries et al., Nucl. Fusion **56** (2016) 56026007, [2] R.J. La Haye et al., Nucl. Fusion **46** (2006) 451, [3] Chang, Z. et al., Nucl. Fusion **36** (1996) 219, [4] M.F.F. Nave, J.A. Wesson, Nucl. Fusion **30** (1990) 2575, [5] D.A. Gates et al., Nucl. Fusion **36** (1996) 273, [6] N.C. Logan et al., Plasma Phys. Control. Fusion **52** (2010) 045013

First author would like to thank ASDEX Upgrade team members that contributed to the here presented work, especially to M. Maraschek, A. Gude, G. Tardini , T. Odstrčil (former AUG team member) and R. McDermott.

[1]*Department of Applied Physics, Ghent University, Sint-Pietersnieuwstraat 41, B-9000 Ghent, Belgium*
[2]*Max-Planck-Institut für Plasmaphysik, 85748 Garching, Germany*
[3]*ITER Organization, Route de Vinon sur Verdon, CS 90 046, 13067 St Paul Lez Durance, Cedex, France*
[4]*Institute of Plasma Physics of the CAS, Za Slovankou 1782/3, 182 00, Prague, Czech Republic*
[5]*Faculty of Mathematics and Physics, Charles University, Prague, Czech Republic*
[6]*Laboratory for Plasma Physics, Royal Military Academy (LPP-ERM/KMS), B-1000 Brussels, Belgium*
veronika.klevarova@ipp.mpg.de

This work was supported by the European Commission and carried out within the frameworks of the Erasmus Mundus International Doctoral College in Fusion Science and Engineering (FUSION-DC) and of the EUROfusion Consortium and has received funding from the Euratom research and training programme 2014-2018 under grant agreement No 633053. The views and opinions expressed herein do not necessarily reflect those of the ITER Organization or the European Commission.
** See the author list of "X. Litaudon et al Nucl. Fusion **57** 102001 (2017)"*
*+ See the author list of "H. Meyer et al Nucl. Fusion **57** 102014 (2017)"*